

# Materials Advances

Accepted Manuscript

This article can be cited before page numbers have been issued, to do this please use: M. Arshad, M. Hassan, A. Rodriguez-Urbe, A. K. Mohanty and M. Misra, *Mater. Adv.*, 2026, DOI: 10.1039/D6MA00115G.



This is an Accepted Manuscript, which has been through the Royal Society of Chemistry peer review process and has been accepted for publication.

Accepted Manuscripts are published online shortly after acceptance, before technical editing, formatting and proof reading. Using this free service, authors can make their results available to the community, in citable form, before we publish the edited article. We will replace this Accepted Manuscript with the edited and formatted Advance Article as soon as it is available.

You can find more information about Accepted Manuscripts in the [Information for Authors](#).

Please note that technical editing may introduce minor changes to the text and/or graphics, which may alter content. The journal's standard [Terms & Conditions](#) and the [Ethical guidelines](#) still apply. In no event shall the Royal Society of Chemistry be held responsible for any errors or omissions in this Accepted Manuscript or any consequences arising from the use of any information it contains.

## Data Availability Statement

The datasets supporting the findings of this study are available from the corresponding author upon reasonable request. All data generated or analyzed during this study, including raw experimental results, characterization files (e.g., FTIR, TGA, DSC, NMR) and mechanical testing data have been archived and can be shared in compliance with journal policy. No publicly archived datasets were used in this research.



# 1 Epoxidized Camelina Oil as a Renewable Plasticizer to Develop Highly 2 Toughened and Flexible Polylactic Acid Films

3  
4 Muhammad Arshad<sup>a</sup>, Malik Hassan <sup>a,b</sup>, Arturo Rodriguez Uribe<sup>a</sup>, Amar K. Mohanty<sup>a,b\*</sup>,  
5 Manjusri Misra<sup>a,b\*</sup>  
6

7 <sup>a</sup>*Bioproducts Discovery and Development Centre, Department of Plant Agriculture, University  
8 of Guelph, Crop Science Building, Guelph, Ontario, N1G 2W1, Canada*

9 <sup>b</sup>*Department of Interdisciplinary Engineering, College of Engineering, University of Guelph,  
10 Thornbrough Building, Guelph, Ontario N1G 2W1, Canada*

11  
12 **\*Corresponding Authors:** [mohanty@uoguelph.ca](mailto:mohanty@uoguelph.ca) ; [mmisra@uoguelph.ca](mailto:mmisra@uoguelph.ca)  
13

## 14 Abstract

15 This study investigates the influence of epoxidized camelina oil (ECO) as a plasticizer on the  
16 the thermal behavior, mechanical performance, and morphological features of polylactic acid  
17 (PLA). ECO was incorporated into PLA at 5%, 10%, and 15% by weight, and its effect on  
18 elongation at break, impact resistance, modulus, and fracture behavior was evaluated. Nuclear  
19 Magnetic Resonance (NMR) spectroscopy confirmed the successful epoxidation of camelina oil,  
20 with the disappearance of olefinic proton signals and the appearance of oxirane group signals,  
21 validating the high degree of functionalization. Similarly, Fourier-transform infrared (FTIR)  
22 spectroscopy confirmed the conversion of double bonds into epoxide groups through the  
23 appearance of oxirane peaks and the disappearance of -C=C-H stretching vibrations, along with  
24 shifts in PLA carbonyl peaks, indicating hydrogen bonding and strong intermolecular interactions.  
25 Mechanical testing showed that addition of 10% ECO significantly enhanced the material  
26 properties, with a 1680% increase in elongation at break and a 24% improvement in impact  
27 strength compared to neat PLA, indicating substantial improvements in flexibility and toughness.  
28 SEM micrographs of tensile and impact fracture surfaces confirmed the transition from brittle to  
29 ductile failure with increasing ECO content, showing rougher surfaces, localized plastic  
30 deformation, and reduced crack propagation. Thermal analysis demonstrated a reduction in glass  
31 transition temperature with ECO addition, further validating its role as a plasticizer. This study  
32 demonstrates that ECO effectively tailors the properties of PLA, making it suitable for applications  
33 requiring improved ductility, toughness, and energy absorption, such as packaging and biomedical  
34 materials.



1 **Keywords:** Polylactic acid (PLA), Epoxidized Camelina Oil (ECO), Plasticizer, Elongation at  
2 Break, Impact Strength, Energy Absorption

#### 4 **Highlights**

- 5 • Epoxidized camelina oil (ECO) was successfully utilized as a renewable plasticizer to  
6 enhance the properties of polylactic acid (PLA).
- 7 • Nuclear Magnetic Resonance (NMR) confirmed the disappearance of olefinic protons  
8 and appearance of oxirane protons, while ATR-FTIR identified oxirane peaks and PLA  
9 carbonyl shifts, validating strong ECO-PLA interactions.
- 10 • Mechanical testing showed a 1680% increase in elongation at break and a 25% rise in  
11 impact strength, transitioning PLA from brittle to ductile.
- 12 • SEM revealed rougher fracture surfaces with fibrillation, indicating enhanced energy  
13 absorption and chain mobility in ECO-PLA blends.
- 14 • ECO effectively reduced PLA's glass transition temperature, improving flexibility and  
15 toughness for packaging and biomedical applications.

#### 17 **1. Introduction**

18 In recent years, an increased concern has been seen on climate change by the government,  
19 industries, and communities due to the higher rate of greenhouse gas emissions resulting from non-  
20 renewable disposal wastes and emphasized their replacement with renewable resources or bio-  
21 based materials[1–3]. Polylactic acid (PLA) offers an attractive "green" alternative to petroleum-  
22 based plastics due to its renewable origin from the fermentation of agricultural carbohydrates. With  
23 similar performance properties to many commodity plastics, PLA has been found to degrade  
24 within 3-6 months under composting conditions. In order for polymer to be considered  
25 compostable, greater than 90% weight loss must occur within 180 days, the degradation process  
26 should not produce any toxic by-products, and the final compost should be able to support plant  
27 growth [4]. PLA is said to meet these criteria, making it an ideal candidate to reduce environmental  
28 impact. Due to its biodegradability, high mechanical strength and biocompatibility, it is an  
29 attractive candidate in numerous industrial applications such as textiles, packaging, biomedical  
30 and many others [5–7]. However, its low toughness and elongation at break limit its potential  
31 applications to serve as a substitute of fossil-derived materials and products[8,9]. Hence,  
32 improving the toughness and ductility of PLA is an ultimate requirement for its application in the  
33 development of bio-based materials. In this regard, numerous techniques and strategies such as



1 copolymerization, blending with other polymers, PLA modification using plasticizers, and  
2 incorporating fillers, have been employed to toughen PLA [10,11].

3 Plasticizers play a dual role in polymer systems: they not only improve processability but also  
4 enhance the flexibility and ductility of rigid, glassy polymers. For PLA, an ideal plasticizer should  
5 effectively lower its glass transition temperature ( $T_g$ ), be biodegradable, non-toxic, non-volatile,  
6 and exhibit minimal leaching or migration over time [12–14]. The efficiency of a plasticizer is  
7 typically assessed by its ability to reduce  $T_g$  and improve tensile toughness, which depends on its  
8 compatibility with the polymer matrix, molecular weight, and loading concentration [15–17].

9 Plant oils being renewable, non-toxic, inexpensive, abundant, and biodegradable [18,19] are  
10 considered as a suitable green feedstock and alternative to petroleum based additives/plasticizer to  
11 serve as a toughness modifier for PLA. Although, different derivatized forms of vegetable oils  
12 such as epoxidized palm oil and soybean [20–23], maleinized linseed, hempseed, and cotton seed  
13 oil [24–26], and acrylated epoxidized soybean oil [21] have been reported as a plasticizer to  
14 improve PLA toughness. However, most vegetable oil derivatives have not provided the desired  
15 toughness due to their incompatibility with PLA [27,28].

16 Camelina oil presents several advantages that make it a promising precursor for renewable  
17 plasticizers. It is a non edible oilseed crop that grows well on marginal land with low fertilizer and  
18 water requirements, which reduces competition with food resources and improves its overall  
19 sustainability profile [29]. The oil contains a high proportion of polyunsaturated fatty acids,  
20 typically 50%, with alpha-linolenic acid (30–40%) as the dominant component [30]. This high  
21 level of unsaturation provides a large number of reactive carbon carbon double bonds, which  
22 enables efficient conversion to oxirane rings during epoxidation and results in a high epoxy group  
23 density per gram of product. A high epoxy density strengthens the interaction between the  
24 modified oil and polar polymer matrices such as PLA and improves plasticization performance.  
25 Previous studies have shown that epoxidized oils with higher unsaturation produce more effective  
26 toughening and flexibility improvements in biodegradable polymers because of their higher  
27 reactivity and stronger secondary interactions with the polymer chains. These characteristics  
28 highlight the potential of camelina oil as a suitable and sustainable feedstock for the development  
29 of renewable plasticizers.



1 In this study, camelina oil, sourced from “*Camelina Sativa*, a non-food oilseed crop, was  
2 epoxidized and utilized as a plasticizer to enhance ductility and toughness of PLA. Camelina oil  
3 with high unsaturated content (90%) was epoxidized through treatment with hydrogen peroxide  
4 and formic acid, using a catalyst to facilitate the reaction [31,32]. The developed epoxidized  
5 camelina oil (ECO) after characterization with Fourier Transform Infrared (FTIR) and Nuclear  
6 Magnetic Resonance (NMR) was used as plasticizer in PLA. Various ratios of ECO (5, 10 and  
7 15%) as a plasticizer were blended with PLA using injection molding. The fabricated blends of  
8 epoxidized camelina oil in PLA (ECO-PLA) were investigated for thermal and mechanical  
9 properties to see the impact of plasticizer on the improvement in toughness and ductility of PLA.

## 10 2. Materials and Methods

### 11 2.1. Materials

12 Camelina oil was obtained from Smart Earth Company (Saskatoon, Canada). Polylactic acid  
13 (PLA) (Ingeo 3251D) was supplied by NatureWorks and has a melting temperature range between  
14 155 °C and 170 °C. Its melt flow rate, at 190 °C under a load of 2.16 kg, falls within the range of  
15 30 to 40 g/10 min. Additional chemicals, including Amberlite-IR120 ion exchange resin (hydrogen  
16 form, Fluka, St. Louis, MO, USA), formic acid (98%, EMD Millipore), hydrogen peroxide (30  
17 wt.% in water), toluene ( $\geq 99.5\%$ ), sodium chloride ( $\geq 99.0\%$ ), and anhydrous magnesium sulfate  
18 ( $\geq 97\%$ ), were purchased from Sigma Aldrich and used without further modification.

### 19 2.2. Epoxidation of Camelina Oil (ECO)

20 The camelina oil was epoxidized using a method adapted from a previously reported procedure  
21 [33]. Briefly, 200 g of camelina oil, 20g amberlite ion exchange resin-H<sup>+</sup>, and 33.3 g of formic  
22 acid, were taken and dissolved in 150 mL toluene. 200 mL of H<sub>2</sub>O<sub>2</sub> solution (30 wt. %) was added  
23 dropwise into the flask in about 20 minutes. Caution should be taken due to the highly exothermic  
24 nature of the reaction. After addition of H<sub>2</sub>O<sub>2</sub>, the temperature was maintained at 60 °C, while  
25 applying heat source. The reaction was completed in 3 hours as checked by FTIR. Upon  
26 completion, the reaction mixture was cooled down to room temperature, and the resin was removed  
27 by filtration. The organic layer was washed three times with 750 mL of water, and 100 mL of brine  
28 added to separate any emulsions. The washed organic layer was dried using anhydrous magnesium



1 sulfate, filtered, and evaporated using rotary vapor. The process yielded a light-yellow liquid  
2 product weighing 201 g.

3 In this study, Amberlite IR120 in the hydrogen form was selected as the catalyst for the epoxidation  
4 of camelina oil because it provides strong protonic acidity, high catalytic efficiency, and  
5 convenient handling during the Prilezhaev type epoxidation reaction. The solid resin promotes the  
6 in situ formation of performic acid from formic acid and hydrogen peroxide, which then reacts  
7 with the unsaturated bonds in camelina oil to form oxirane rings. Unlike liquid mineral acids such  
8 as sulfuric acid, Amberlite does not create corrosion concerns, does not require neutralization after  
9 the reaction, and reduces the formation of unwanted side products, including excessive ring  
10 opening or oxidative degradation. The heterogeneous nature of the resin allows simple removal by  
11 filtration and enables reuse in subsequent reactions, which improves the sustainability of the  
12 process. These advantages, combined with reliable catalytic activity and minimal environmental  
13 impact, make Amberlite IR120 an effective and practical catalyst for producing highly epoxidized  
14 camelina oil.

### 15 2.3. Fabrication of ECO-PLA Blends

16 The PLA pellets and ECO were subjected to drying in an oven at 80 °C overnight to achieve a  
17 moisture content below 0.1%. The blends of PLA and ECO were prepared using a DSM Xplore  
18 15 mL laboratory-scale microcompounder (Xplore Instruments BV, The Netherlands), equipped  
19 with co-rotating twin screws of 150 mm length and an aspect ratio (L/D) of 18, and a barrel  
20 comprising three independently controlled heating zones. For extrusion, PLA and ECO (5 wt.%,  
21 10 wt.%, and 15 wt.%) were manually mixed and directly fed into the barrel. The compounding  
22 was performed at a processing temperature of 180 °C and a screw speed of 100 rpm. The materials  
23 were retained within the barrel for a fixed residence time of 2 minutes to ensure complete melt  
24 homogenization before being transferred directly into the injection molding chamber, which was  
25 set at 40 °C. The prepared blends were labeled as 5% ECO-PLA, 10% ECO-PLA, and 15% ECO-  
26 PLA, respectively. A neat PLA control sample (without ECO) was also processed under identical  
27 conditions for comparison.

## 28 3. Characterization Techniques

### 29 Fourier-transform infrared (FTIR) Analysis



1 FTIR analysis was performed on the prepared samples using a Nicolet 6700 ATR-FTIR  
2 spectrometer (ThermoScientific, USA). The spectra were recorded at a resolution of  $4\text{ cm}^{-1}$  across  
3 a wavenumber range of  $500\text{--}4000\text{ cm}^{-1}$ , with an average of 64 scans per spectrum.

#### 4 **Nuclear Magnetic Resonance (NMR) Analysis**

5 NMR spectra were recorded on a Bruker AVANCE III spectrometer operating at 600 MHz,  
6 equipped with a 5-mm TCI cryoprobe. Deuterated chloroform ( $\text{CDCl}_3$ ) was used as the solvent for  
7 all experiments.

#### 8 **Thermal Analysis**

9 Differential scanning calorimetry (DSC) was performed using a Q200 system (TA Instruments,  
10 New Castle, DE, USA), which included a cooling system, to determine the melting, crystallization,  
11 and glass transition temperatures of the samples. Specimens weighing 5–10 mg were sealed in  
12 aluminum pans for the analysis. The procedure commenced with an initial heating cycle from  $-70$   
13  $^{\circ}\text{C}$  to  $200\text{ }^{\circ}\text{C}$  at a heating rate of  $10\text{ }^{\circ}\text{C}/\text{min}$ , followed by an isothermal hold for 2 minutes at  $200$   
14  $^{\circ}\text{C}$ . This was followed by a cooling cycle to cool the sample to  $-70\text{ }^{\circ}\text{C}$  from  $200\text{ }^{\circ}\text{C}$  at a rate of  $5$   
15  $^{\circ}\text{C}/\text{min}$ , with an additional isothermal hold at  $-70\text{ }^{\circ}\text{C}$  for 2 minutes. Finally, a second heating cycle  
16 was carried out under the same conditions as the first heating cycle.

17 Thermogravimetric analysis (TGA) was performed using a Q500 thermogravimetric analyzer (TA  
18 Instruments, Delaware, USA) to examine the thermal degradation behavior of the samples.  
19 Specimens with a mass of 10-20 mg were heated from room temperature to  $600\text{ }^{\circ}\text{C}$  at a rate of  $10$   
20  $^{\circ}\text{C}/\text{min}$ , while maintaining a nitrogen flow of  $60\text{ mL}/\text{min}$ .

#### 21 **Dynamic Mechanical Analysis (DMA)**

22 DMA was performed using a Q800 Dynamic Mechanical Analyzer (TA Instruments, USA) to  
23 evaluate the viscoelastic properties of neat PLA and ECO-PLA blends. Rectangular specimens ( $35$   
24  $\text{mm} \times 12\text{ mm} \times 3\text{ mm}$ ) were tested using a dual cantilever clamp in multi-frequency strain mode.  
25 The analysis was conducted at a fixed frequency of  $1\text{ Hz}$  and a displacement amplitude of  $20\text{ }\mu\text{m}$ ,  
26 ensuring that measurements were taken within the linear viscoelastic region (LVR). The test began  
27 with temperature equilibration at  $-35\text{ }^{\circ}\text{C}$ , followed by heating to  $120\text{ }^{\circ}\text{C}$  at a rate of  $3\text{ }^{\circ}\text{C}/\text{min}$  under  
28 multi-frequency strain mode. Throughout the test, the storage modulus ( $E'$ ), loss modulus ( $E''$ ),  
29 and damping factor ( $\tan \delta$ ) were recorded. The glass transition temperature ( $T_g$ ) was determined



1 from the peak of the  $\tan \delta$  curve, and the effect of ECO concentration on molecular mobility was  
2 analyzed from shifts in both Tg and modulus behavior.

### 3 **Mechanical Characterization**

4 Mechanical testing, including tensile, flexural, and impact tests, was conducted to evaluate the  
5 effects of ECO on the properties of PLA. All tests were performed on five replicates for each  
6 formulation to ensure reliability and account for variability. Tensile testing was carried out using  
7 a universal testing machine (Instron 3382, Massachusetts, USA), equipped with a 5kN load cell,  
8 following ASTM D638 standard [34]. The tests were conducted at a crosshead speed of 5 mm/min  
9 using dog-bone-shaped specimens to measure tensile strength, elongation at break, and modulus.  
10 Flexural tests were performed according to ASTM D790 standard [35], using the same testing  
11 machine under identical environmental conditions. Impact tests were conducted on notched Izod  
12 specimens using an impact tester (Zwick/Roell HIT25P, Ulm, Germany) in compliance with  
13 ASTM D256 standard [36]. A 2.75 J capacity pendulum hammer was used for all tests. All tests  
14 were performed on five replicates, and the reported values represent the average results.

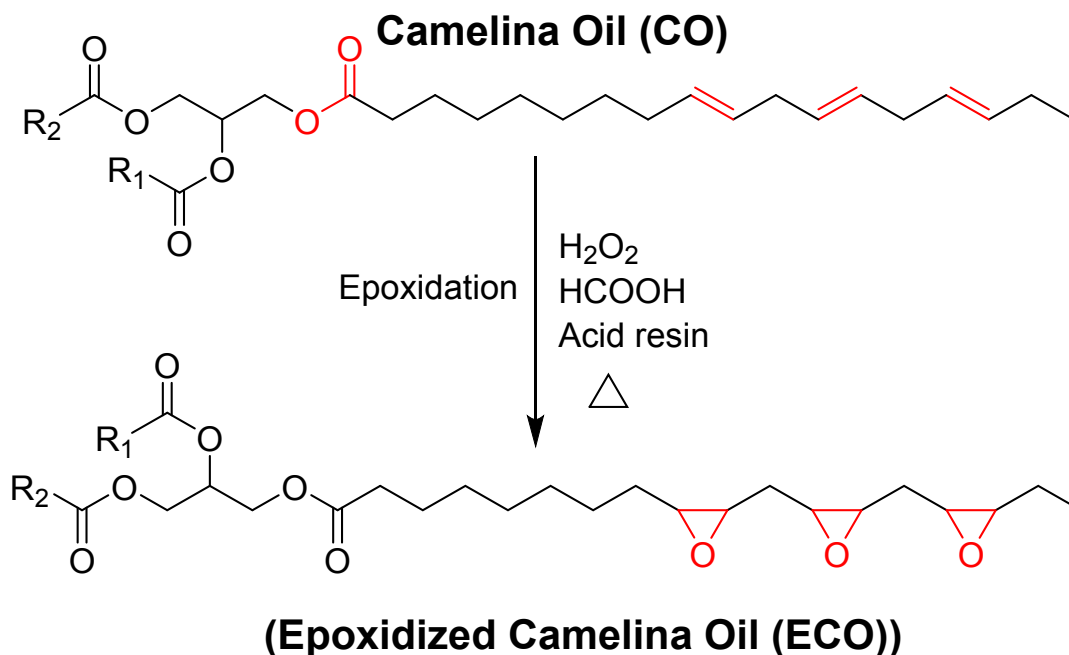
### 15 **Morphological analysis**

16 The tensile and impact-fractured surfaces of PLA and ECO-PLA samples were analyzed using  
17 scanning electron microscopy (SEM) (Phenom-World, BV, North Brabant) to examine their  
18 morphological characteristics. A thin gold coating was applied to the surfaces to improve  
19 conductivity, and the analysis was performed at an operating voltage of 10 kV.

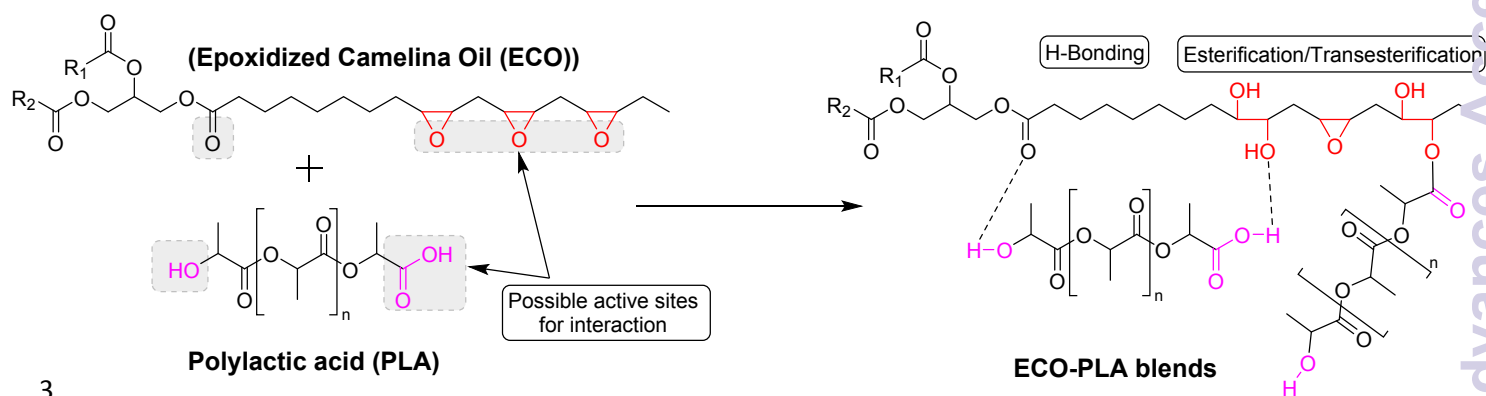
## 20 **4. Results and Discussion**

21 Camelina oil, known for its high unsaturated content, was epoxidized using hydrogen peroxide  
22 and formic acid, with Amberlite ion exchange resin-H<sup>+</sup> serving as the catalyst. The resulting  
23 epoxidized oil was then employed as a plasticizer for PLA. Various proportions of ECO (5%, 10%,  
24 and 15%) were blended with PLA through injection molding to develop the desired blends.  
25 Furthermore, the characterization of the synthesized ECO and the evaluation of the developed  
26 blends for their thermal and chemical properties are discussed in the subsequent sections. Scheme  
27 1 illustrates the epoxidation process of camelina oil, while scheme 2 depicts the proposed chemical  
28 interactions between ECO and PLA, potentially involving hydrogen bonding and  
29 esterification/transesterification.





1  
2 Scheme 1: Epoxidation of camelina oil in the presence of acidic ion exchange resin.



3  
4 Scheme 2: Proposed chemical interactions of ECO with PLA via hydrogen bonding and or  
5 esterification/transesterification.

#### 7 4.1. FTIR Analysis

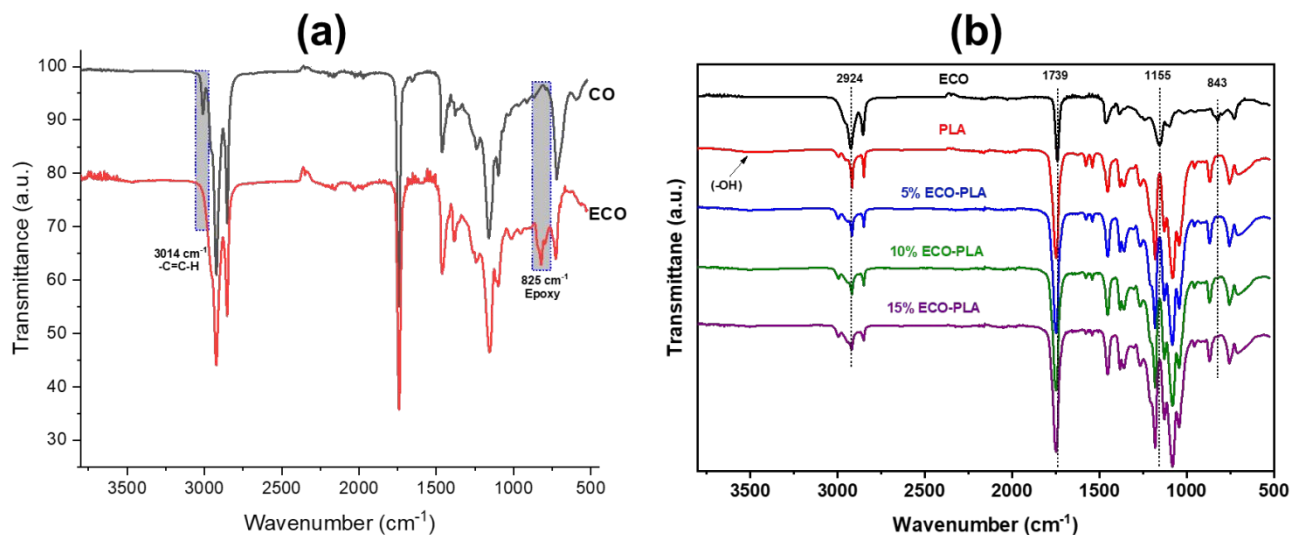
8 FTIR spectroscopy provided essential insights into the molecular interactions between ECO and  
9 PLA, confirming both the successful epoxidation of camelina oil and the plasticizing effect of  
10 ECO in the blends. For the pure ECO sample, the epoxidation was confirmed by the disappearance  
11 of the C=C-H stretching peak at around  $3014\text{ cm}^{-1}$ , characteristic of camelina oil's unsaturated  
12 double bonds as can be seen in Figure 1(a). This was replaced by a new peak at approximately  $825$   
13  $\text{cm}^{-1}$ , associated with the symmetric and asymmetric stretching of the oxirane (epoxide) ring,



1 indicating successful conversion of double bonds to reactive epoxide groups [37,38]. These  
2 epoxide groups are important for compatibility with PLA, as they facilitate intermolecular  
3 interactions and potential chemical reactions with PLA functional groups. In the ECO-PLA blends  
4 (Figure 1(b)), several notable changes in the FTIR spectrum further highlighted the interactions  
5 between ECO and PLA. The carbonyl (C=O) stretching peak of PLA, typically observed around  
6  $1750\text{ cm}^{-1}$ , shifted slightly to lower wavenumbers in the ECO-PLA blends, especially at higher  
7 ECO content (10% and 15%). This shift suggests that hydrogen bonding occurs between PLA's  
8 carbonyl groups and hydroxyl groups formed from the epoxide ring opening in ECO, which  
9 reduces the vibrational energy and shifts the absorption frequency of the carbonyl group [39,40].  
10 A broad band appeared in the  $3500\text{--}3200\text{ cm}^{-1}$  region, corresponds to O-H stretching vibrations,  
11 indicating the presence of hydroxyl groups formed as a result of epoxide ring opening in ECO  
12 [41]. The presence of these hydroxyl groups, likely forming hydrogen bonds with PLA, confirms  
13 the strong interaction between ECO and PLA [42]. These interactions contribute to the plasticizing  
14 effect observed in the blends, where the increased mobility of PLA chains results in improved  
15 flexibility and toughness.

16 Additionally, the FTIR spectrum showed changes in the aliphatic C-H stretching region ( $2950\text{--}$   
17  $2850\text{ cm}^{-1}$ ) as ECO content increased, reflecting the introduction of more aliphatic chains from  
18 ECO. While the intensity of these peaks did not significantly increase, their presence confirms the  
19 successful integration of ECO, which contributes to improved ductility and reduced stiffness in  
20 the blends [43].





1  
2 Figure 1: ATR-FTIR spectra of (a) CO and ECO; (b) neat PLA, 5% ECO-PLA, 10% ECO-PLA,  
3 and 15% ECO-PLA.

#### 4 5 **4.2. NMR Analysis**

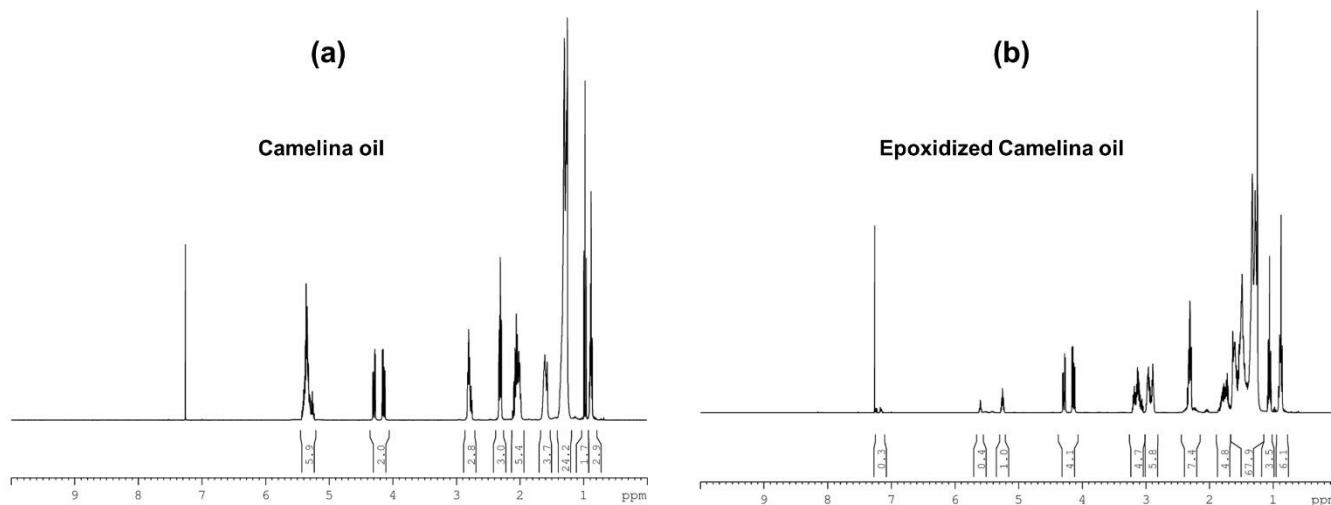
6 Figure 2 highlights the  $^1\text{H}$  NMR spectra of camelina oil (CO) before and after epoxidation,  
7 illustrating the successful transformation of unsaturated double bonds into oxirane (epoxide)  
8 groups. In the spectrum of unmodified CO, prominent peaks were observed at 5.3–5.5 ppm,  
9 corresponding to the protons of olefinic double bonds ( $-\text{HC}=\text{CH}-$ ). The disappearance of peaks  
10 associated with double bonds in the ECO spectrum indicates their successful conversion into  
11 oxirane groups. Simultaneously, the peaks appearance in the range of 2.8–3.2 ppm corresponds to  
12 protons in the oxirane rings, confirming the formation of epoxide groups. This spectral shift is a  
13 definitive indicator of the successful epoxidation process [37]. In the aliphatic region, signals in  
14 the range of 0.8–2.5 ppm correspond to the methylene ( $-\text{CH}_2-$ ) and methyl ( $-\text{CH}_3$ ) groups of the  
15 fatty acid chains [44]. These peaks are present in both spectra, indicating that the hydrocarbon  
16 backbone remains intact during the epoxidation process. While their intensities remain largely  
17 unchanged, the slight differences in peak shape suggest minor structural rearrangements in the  
18 chains caused by the introduction of epoxide groups. The glycerol backbone protons ( $-\text{CH}_2-\text{O}-$ )  
19 are observed in the region of 4.1–4.3 ppm in the CO spectrum [45]. In the ECO spectrum, these  
20 peaks appear shifted and slightly less intense, likely due to changes in the electronic environment  
21 caused by the epoxidation. Additionally, a broad peak emerges around 3.3–3.5 ppm in the ECO  
22 spectrum, corresponding to hydroxyl protons formed due to partial ring-opening reactions of the



1 epoxide groups. These hydroxyl groups enhance hydrogen bonding with the carbonyl groups of  
2 PLA, improving the miscibility and interfacial interactions in ECO-PLA blends.

3 Furthermore, the absence of peaks in the 5.3–5.5 ppm region of the ECO spectrum indicates that  
4 the olefinic double bonds were largely consumed during epoxidation, consistent with the 92.6%  
5 conversion calculated from  $^1\text{H}$  NMR integration. Based on this conversion, approximately 5.1  
6 mmol of epoxide groups per gram of sample were obtained.[46] Similarly, in another study, the  
7 epoxidation percentage was determined to be 94.5%, based on the vinyl signals observed between  
8 5.3 and 5.5 ppm in the  $^1\text{H}$  NMR spectrum [47]. The significant reduction of these peaks in the  
9 ECO spectrum indicates that most of the double bonds have been successfully converted to  
10 epoxide groups. The absence of residual olefinic protons and the presence of strong oxirane proton  
11 peaks indicate a high degree of epoxidation, crucial for the enhanced plasticizing efficiency of  
12 ECO. The density of oxirane groups facilitates intermolecular interactions with PLA, including  
13 hydrogen bonding and esterification reactions, which improve the ductility and toughness of PLA,  
14 as previously discussed by Chieng et al. [41] and Thuy et al. [48].

15



16

17

Figure 2:  $^1\text{H}$  NMR spectra of (a) CO, and (b) ECO.

18 The FTIR and NMR results not only confirm the formation of oxirane rings in the epoxidized  
19 camelina oil but also provide evidence for chemical interactions between the epoxidized oil and  
20 PLA chains. The downward shift of the PLA carbonyl absorption band and the appearance of a  
21 broad hydroxyl region indicate the presence of hydrogen bonding between the hydroxyl groups  
22 formed during partial ring opening of the epoxy groups and the carbonyl oxygen atoms of PLA.



1 Hydrogen bonding increases temporary physical cross links that restrict local chain packing but  
2 simultaneously increase segmental mobility by weakening the strong intermolecular interactions  
3 that normally lead to brittle fracture in neat PLA. Several studies report that hydrogen bonded  
4 plasticizers reduce the glass transition temperature of PLA by increasing the free volume and  
5 promoting cooperative chain motion, which directly enhances ductility and impact resistance. In  
6 addition to hydrogen bonding, the residual epoxy groups in ECO may undergo limited ester  
7 exchange reactions with the terminal hydroxyl groups of PLA during melt blending. Such reactions  
8 create weakly bonded junction points that improve compatibility and reduce phase separation.  
9 These chemical interactions collectively explain the significant increase in elongation at break and  
10 the transition from brittle to ductile fracture behavior observed in the SEM images. Prior literature  
11 on epoxidized plant oils in PLA systems also shows that strong secondary interactions and partial  
12 ester linkages increase chain mobility and substantially improve toughness, which is consistent  
13 with the mechanical performance trends observed in this study.

#### 14 **4.3. Thermal Analysis**

15 As shown in Figure 3 and Table 1, the DSC thermograms include both the cooling scan and the  
16 second heating scan to illustrate the influence of ECO on the thermal behavior of PLA. The  
17 analysis indicated a progressive reduction in the  $T_g$  of PLA as the ECO content was increased from  
18 5% to 15%. Neat PLA typically has a  $T_g$  around 60°C, a temperature at which the polymer  
19 transitions to a more flexible, rubbery state from a rigid, glassy state. The 5% ECO-PLA blend  
20 showed a  $T_g$  decrease to approximately 55.46°C, while the 10% and 15% ECO-PLA blends  
21 reduced  $T_g$  further to around 53.86°C and 53.62°C, respectively. Similarly, cold crystallization  
22 temperature of pure PLA was reduced from 95.4°C to 91.2°C on incorporation of 5% ECO, while  
23 no significant differences were observed in 10% and 15% ECO-PLA. This downward shift in  $T_g$   
24 and cold crystallization temperature is indicative of the plasticizing effect of ECO, which enhances  
25 the polymer chain mobility [41,49]. Increased chain mobility implies that the polymer can absorb  
26 more stress without fracturing, thereby reducing brittleness and enabling improved flexibility [42].  
27 The melting temperature ( $T_m$ ) showed a slight reduction from neat PLA's typical melting point,  
28 suggesting that the crystalline regions within PLA were somewhat disrupted by the inclusion of  
29 ECO [50].



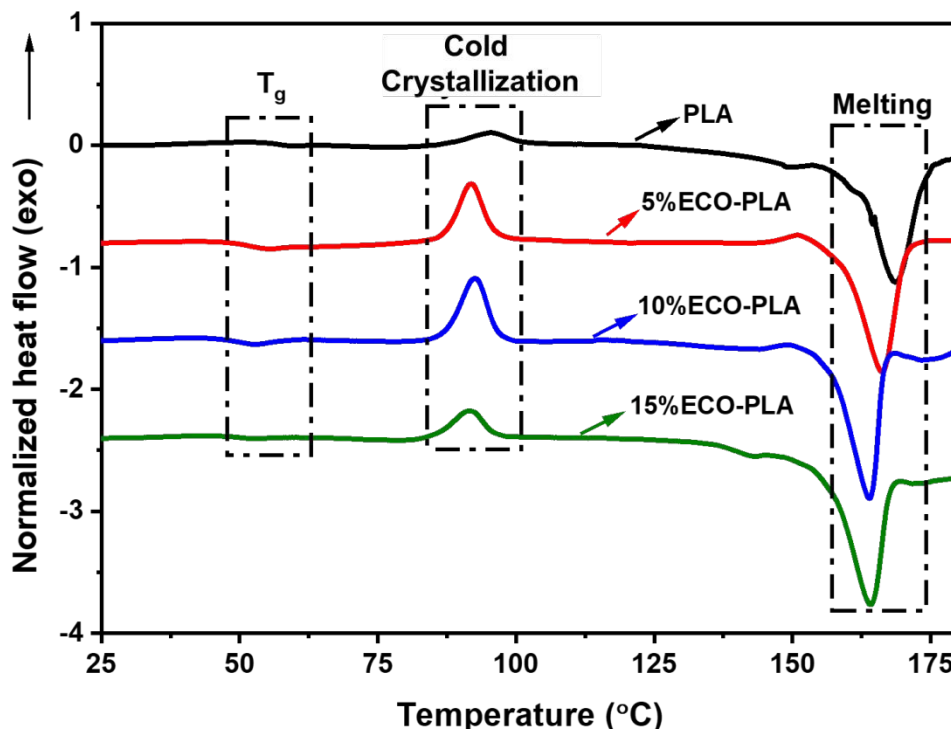


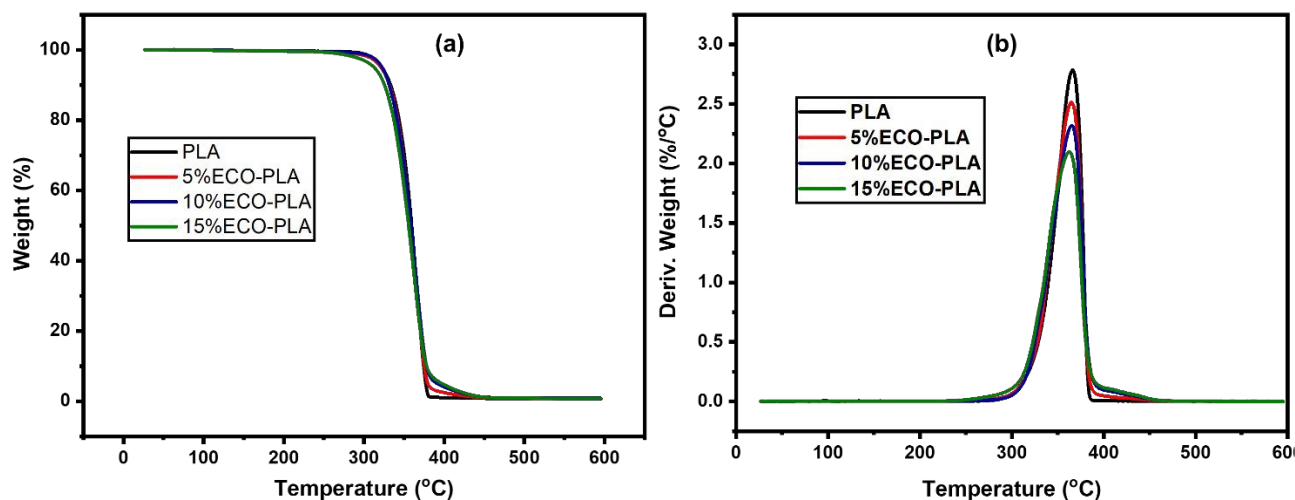
Figure 3: DSC thermograms of neat PLA and its blends containing 5%, 10%, and 15% ECO.

The TGA curve (Figure 4) provides valuable insights into the thermal stability and decomposition behavior of neat PLA and ECO-PLA blends with varying ECO content (5%, 10%, and 15%). In the TGA plot, the neat PLA sample (black line) begins to decompose at a higher onset temperature, underscoring its improved thermal stability in contrast to the ECO-PLA blends. As the ECO content increases, the onset of decomposition shifts slightly to lower temperatures, particularly for the 10% and 15% ECO-PLA blends, as can be seen in Table 1. This shift indicates that the addition of ECO reduces the thermal stability of PLA, likely due to the lower decomposition temperature of ECO and the plasticizing effect. The plasticizer weakens intermolecular forces within the PLA matrix, increases chain mobility, and introduces more thermally labile components, contributing to earlier thermal degradation [51].

All samples exhibit a sharp weight loss around 300°C–350°C, corresponding to the primary decomposition phase of PLA, where rapid depolymerization occurs. This phase results in significant weight loss, primarily due to the breakdown of the polymer backbone into volatile products. While the degradation behavior is consistent across all blends, the weight loss in this region is slightly more pronounced for the 15% ECO-PLA blend, as indicated by its notably lower  $T_{5\%}$  value compared to neat PLA (Table 1). This trend suggests that the increase in content of ECO



1 accelerates thermal decomposition, a behavior commonly observed in plasticized polymer  
2 systems. Plasticizers, having lower thermal stability and increasing the free volume within the  
3 polymer matrix, facilitate earlier chain scission and enhance the rate of decomposition [52,53]. At  
4 higher temperatures, the TGA curves level off, indicating the completion of the decomposition  
5 process. Minimal residual weight remains for both neat PLA and ECO-PLA blends, signifying  
6 almost complete thermal breakdown. This behavior confirms that while the incorporation of ECO  
7 slightly decreases the thermal stability of PLA, the blends still exhibit thermal stability adequate  
8 for most processing and application conditions.



9  
10 Figure 4: TGA curves for neat PLA and PLA-ECO blends (5% ECO-PLA, 10% ECO-PLA, and  
11 15% ECO-PLA)

12  
13 Table 1: Glass transition temperature ( $T_g$ ), onset temperature ( $T_{onset}$ ), degradation temperature  
14 ( $T_{degradation}$ ), and temperature at 5% weight loss ( $T_{5\%}$ ) for PLA and ECO-based blends

Sample	$T_g$	$T_{onset}$	$T_{degradation}$	$T_{5\%}$
PLA	59.41	341.83	366.22	322.80
5%ECO-PLA	55.46	338.72	364.81	321.19
10%ECO-PLA	53.86	337.22	364.96	322.67
15%ECO-PLA	53.62	332.21	362.54	312.59

#### 15 16 4.4. Dynamic Mechanical Properties

17 Dynamic Mechanical Analysis (DMA) was used to evaluate the viscoelastic behavior of ECO-  
18 PLA blends across a temperature range, focusing on how ECO influences the storage modulus  
19 ( $E'$ ), loss modulus ( $E''$ ), and  $\tan \delta$ . These parameters help to understand the elastic and viscous



1 responses of the material, as well as its energy dissipation characteristics, providing insights into  
2 the flexibility and damping capacity of the blends. Figure 5 (a) shows the elastic behavior of the  
3 material as it deforms under an oscillating force. The storage modulus is high in the glassy region,  
4 indicating that the material is rigid. As the temperature increases,  $E'$  decreases, showing the  
5 material's transition from a glassy to a rubbery state. Beyond this region, the storage modulus  
6 began to rise again due to cold crystallization of PLA within the blends. The onset of cold  
7 crystallization shifted to a lower temperature with increasing ECO content, suggesting that ECO  
8 acted as a plasticizing component that enhanced chain mobility and promoted earlier crystallite  
9 formation [54,55]. Figure 5 (b) reflects the viscous behavior of the material, representing the  
10 amount of energy lost as heat during deformation. A peak in the loss modulus usually corresponds  
11 to the  $T_g$ , where the material's damping properties are highest. The addition of ECO has affected  
12 the height and position of this peak, indicating changes in the  $T_g$  and the damping characteristics  
13 of the blend. A peak in the  $\tan \delta$  curve (Figure 5 (c)) is another indicator of the  $T_g$ . Materials with  
14 a higher  $\tan \delta$  at room temperature can be better at absorbing and dissipating energy, such as in  
15 impact-resistant applications. The incorporation of ECO into PLA has led to a higher  $\tan \delta$ ,  
16 suggesting improved energy dissipation capabilities.



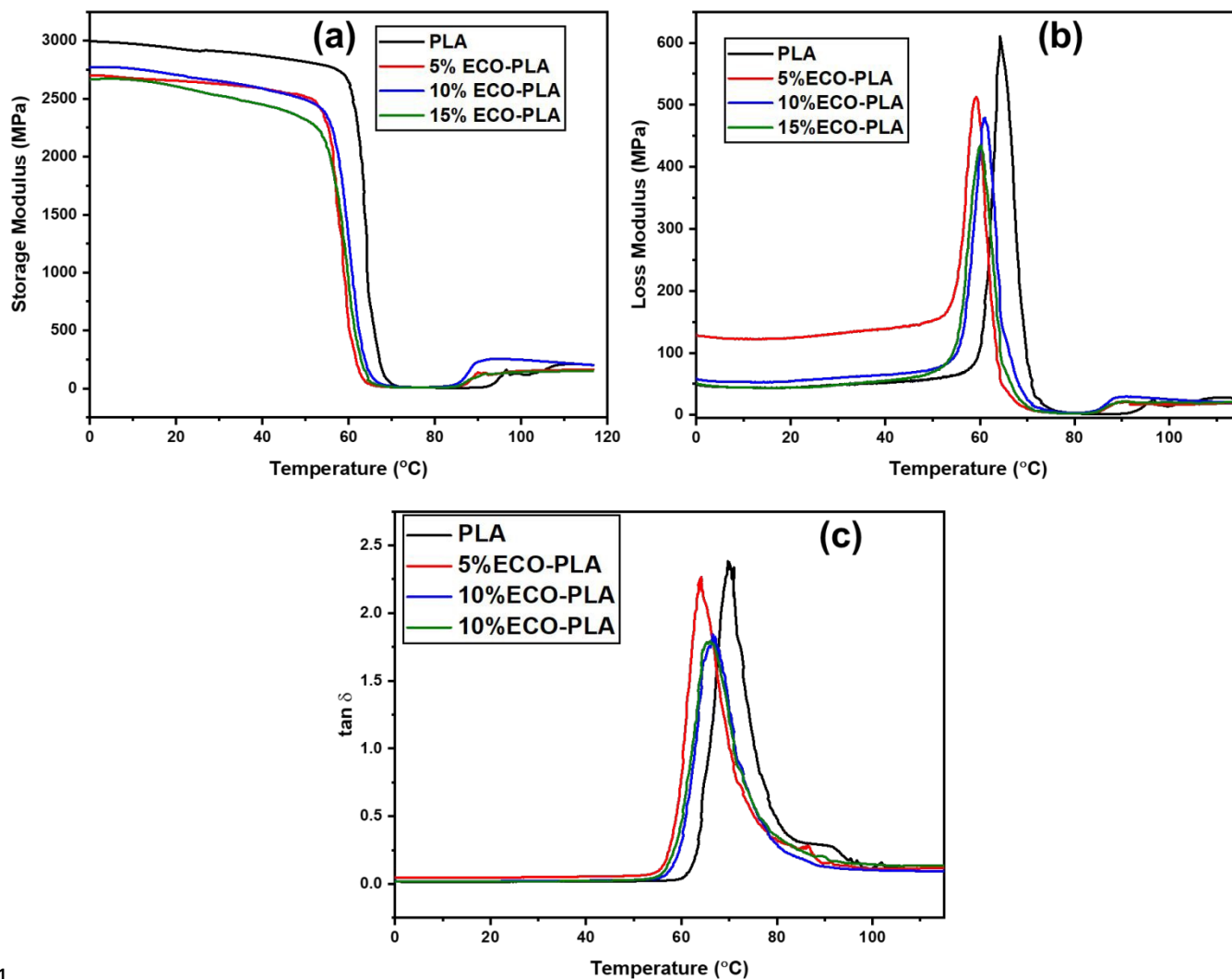


Figure 5: DMA curves of PLA and its blends containing 5%, 10%, and 15% ECO (a) Storage modulus, (b) Loss modulus (c)  $\tan \delta$ .

#### 4.5. Mechanical Properties

Figure 6 (a) presents the stress-strain behavior of neat PLA and PLA-ECO blends with 5%, 10%, and 15% ECO. The stress-strain behavior demonstrates how the material deforms under tensile force, with the slope of the initial linear section indicating stiffness and the area under the curve representing toughness. For pure PLA (0% ECO), the steep initial slope reflects high stiffness and rigidity, but the curve terminates abruptly at maximum stress, indicating brittle failure with minimal deformation. In contrast, as ECO content increases, the curves become less steep and extend further along the strain axis, reflecting reduced stiffness and enhanced ductility. This behavior aligns with lubricity theory, which explains that ECO acts as a lubricant, reducing internal



1 friction and allowing polymer chains to slide past one another more freely. As a result, blends with  
2 higher ECO content exhibit greater chain mobility, enabling them to stretch significantly further  
3 before failure [56]. The increase in elongation at break, as observed in Figure 6 (b), further supports  
4 the gel theory, which states that plasticizers like ECO disrupt and replace strong polymer-polymer  
5 interactions (such as hydrogen bonds and van der Waals forces) with weaker plasticizer-polymer  
6 interactions [41]. This disruption reduces the gel-like structure of the polymer matrix, increasing  
7 flexibility and extensibility. This mechanism has been widely reported in the literature [41,57,58],  
8 where the addition of epoxidized oils to PLA has been shown to increase elongation at break  
9 significantly, transitioning PLA from a brittle to a more ductile one.

10 The tensile and flexural moduli, as shown in Figure 6 (c), decrease with increasing ECO content,  
11 reflecting a reduction in stiffness. This behavior is explained by the gel theory, as the plasticizer  
12 disrupts the dense packing of polymer chains, increasing free volume and chain mobility. This  
13 reduction in intermolecular interactions weakens the polymer network, making the material less  
14 resistant to deformation under tensile and bending loads.

15 As shown in Figure 6 (b), tensile strength, which represents the maximum stress a material can  
16 endure before failure, decreases with higher ECO content. This is due to the reduction in  
17 intermolecular forces within the polymer matrix, which lowers its load-bearing capacity. However,  
18 elongation at break increases dramatically, indicating that the material can deform to a much  
19 greater extent before failure. This trade-off between elongation at break and tensile strength is a  
20 well-documented characteristic of plasticized polymers. Al-Mulla et al. [20] found that adding  
21 epoxidized palm oil to a PLA/polycaprolactone (PCL) blend decreased tensile strength while  
22 markedly increasing elongation at break, indicating improved flexibility.

23 Figure 6 (d) presents the notched impact strength of PLA-ECO blends, which quantifies the  
24 material's ability to absorb and dissipate energy during sudden impact loading. Pure PLA exhibits  
25 relatively low impact strength due to its brittle nature. However, as ECO content increases, impact  
26 strength improves significantly. This improvement can be attributed to ECO's toughening effect,  
27 which enhances energy dissipation by increasing chain mobility and reducing stress concentrations  
28 at the point of impact. The enhanced impact resistance is consistent with lubricity theory, as the  
29 plasticizer reduces friction between polymer chains, allowing for better energy redistribution  
30 during deformation. Several studies have demonstrated this effect. Orue et al. [59] confirmed that



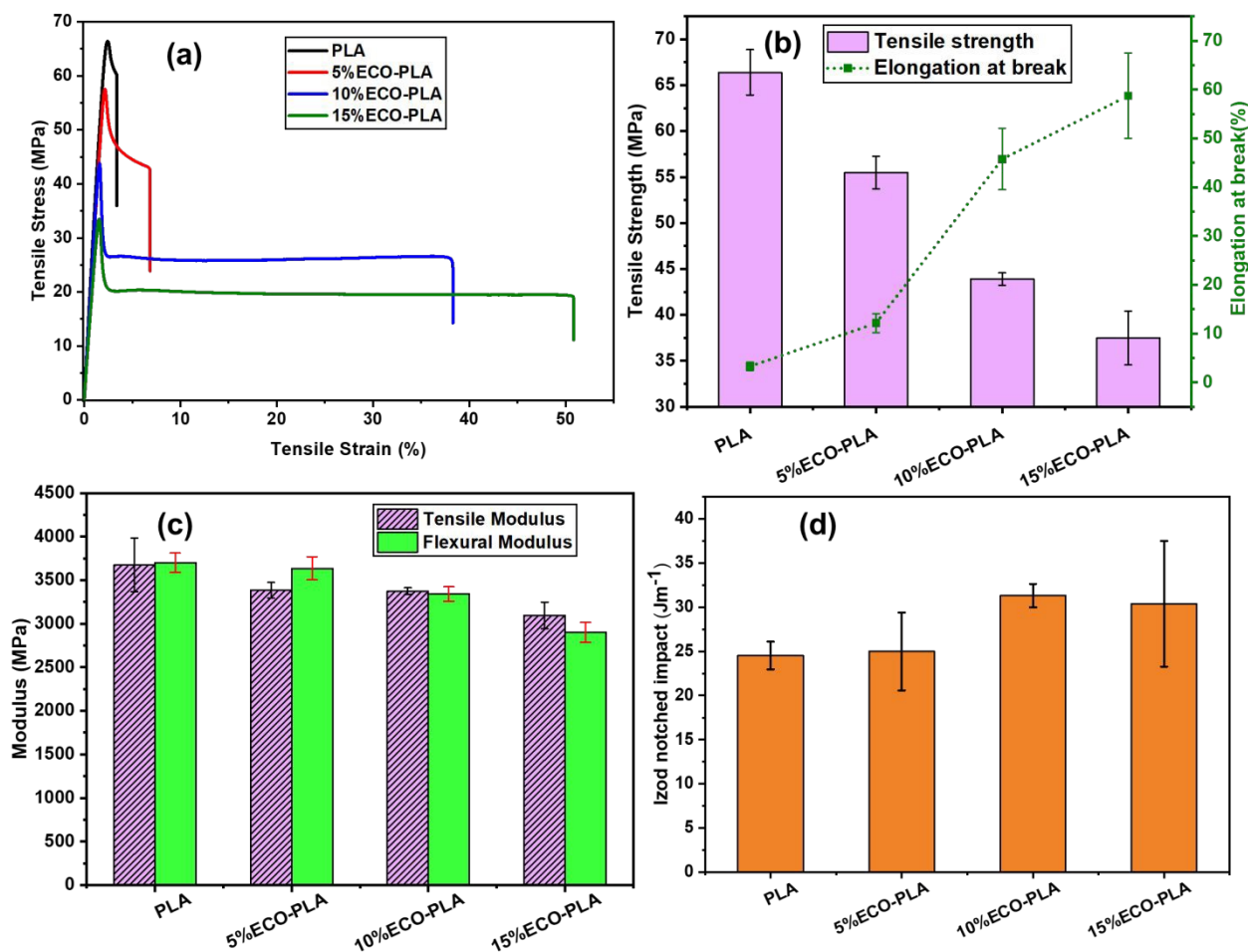
1 epoxidized linseed and soybean oils increased the impact strength of PLA composites, supporting  
2 the toughening mechanism through improved polymer chain mobility. Their findings further prove  
3 that the addition of ECO enhances ductility and stress dissipation. Additionally, Tee et al. [60]  
4 demonstrated that epoxidized palm oil and soybean oil improved PLA's toughness, effectively  
5 reducing stress concentrations and promoting better energy dissipation.

6 While the overall trends show that ECO enhances ductility and impact resistance, the mechanical  
7 response of the 15% ECO blend suggests the onset of over plasticization. The substantial drop in  
8 tensile strength and modulus, combined with the extremely large elongation at break, indicates  
9 that the PLA matrix may approach saturation at this concentration. When saturation occurs, the  
10 polymer loses cohesive strength and deformation becomes dominated by viscous flow rather than  
11 controlled plastic deformation.

12 SEM analysis supports this interpretation. The fracture surface of the 15 % blend shows large  
13 deformation zones, extensive fibrillation, and broad voids, all of which reveal very high chain  
14 mobility and reduced structural integrity. In contrast, the 10% blend shows a more uniform ductile  
15 morphology with finer energy absorbing structures, indicating a more balanced plasticization  
16 effect. The DMA results provide further confirmation. The storage modulus of the 15 % ECO  
17 blend decreases more sharply across the temperature range compared to the 5 and 10 % blends,  
18 and the glass transition temperature shifts to lower values. These observations indicate a highly  
19 softened matrix and reduced intermolecular cohesion, characteristic of over plasticized systems.

20 This behavior is consistent with findings from related studies on epoxidized plant oils in PLA  
21 systems. Prior work has shown that at high plasticizer concentrations, micro scale heterogeneity  
22 and partial phase separation may occur, leading to weaker load bearing capability even though  
23 ductility improves [61–63]. These comparisons suggest that the 10% ECO blend offers the best  
24 balance of strength, toughness, and flexibility, while the 15% blend approaches the upper  
25 compatibility limit for ECO in PLA.





1

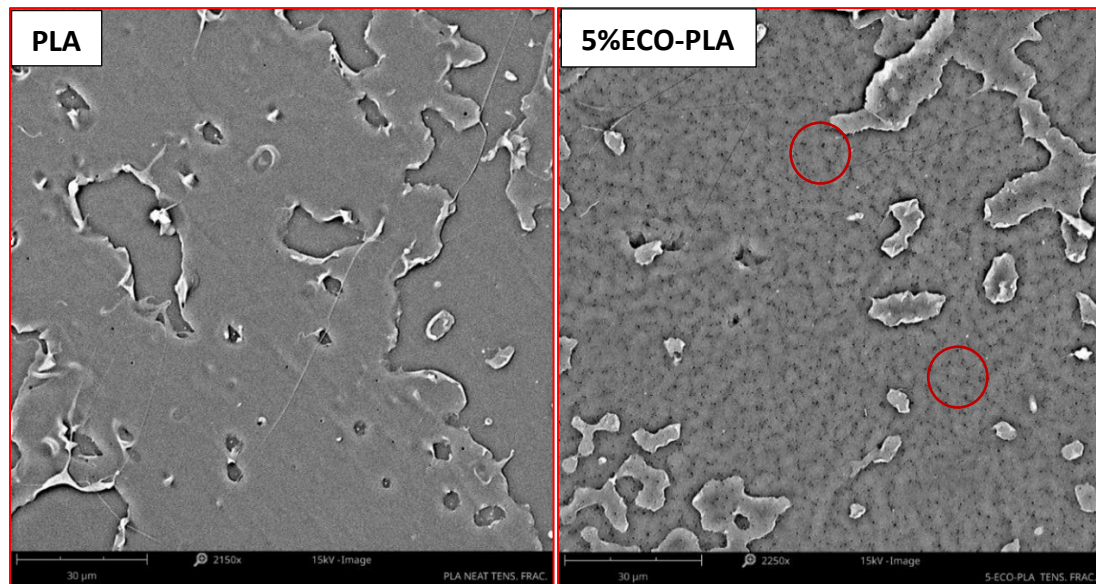
2 Figure 6: (a) Stress-strain curves, (b, c) tensile properties, and (d) Izod notched impact strength  
3 of PLA and its blends containing 5%, 10%, and 15% ECO.

#### 4 4.6. Morphological analysis

5 The SEM micrographs of tensile fractured surfaces for neat PLA, 5%ECO-PLA, 10%ECO-PLA,  
6 and 15%ECO-PLA as shown in Figure 7 demonstrate the progressive impact of ECO on the  
7 fracture morphology of PLA. Neat PLA exhibits a smooth and relatively featureless fracture  
8 surface, characteristic of brittle failure. This is indicative of a rigid material with strong  
9 intermolecular interactions and limited energy dissipation, consistent with its high tensile modulus  
10 and low elongation at break [64]. In contrast, the addition of 5% ECO introduces a rougher fracture  
11 surface with small voids and localized plastic deformation. These features suggest the onset of  
12 ductility as ECO begins to disrupt the rigid PLA matrix, reducing friction between polymer chains  
13 and enabling limited chain mobility. At 10% ECO, the fracture surface shows significant  
14 roughness with pronounced voids and fibrillar structures, indicative of increased cavitation and



1 polymer chain stretching during deformation. This reflects a transition to ductile failure, supported  
2 by the substantial increase in elongation at break observed in the mechanical tests. The addition of  
3 15% ECO further accentuates this trend, with extensive fibrillation and a highly rough fracture  
4 surface, characteristic of highly ductile behavior. The presence of large voids and stretched fibrils  
5 highlights enhanced chain mobility and energy dissipation, although excessive plasticization at  
6 this level may reduce tensile strength due to a less cohesive polymer matrix. These observations  
7 align with the lubricity and gel theories, which describe how ECO disrupts polymer-polymer  
8 interactions, facilitates chain mobility, and transitions the material from brittle to ductile behavior  
9 [41,56].



10



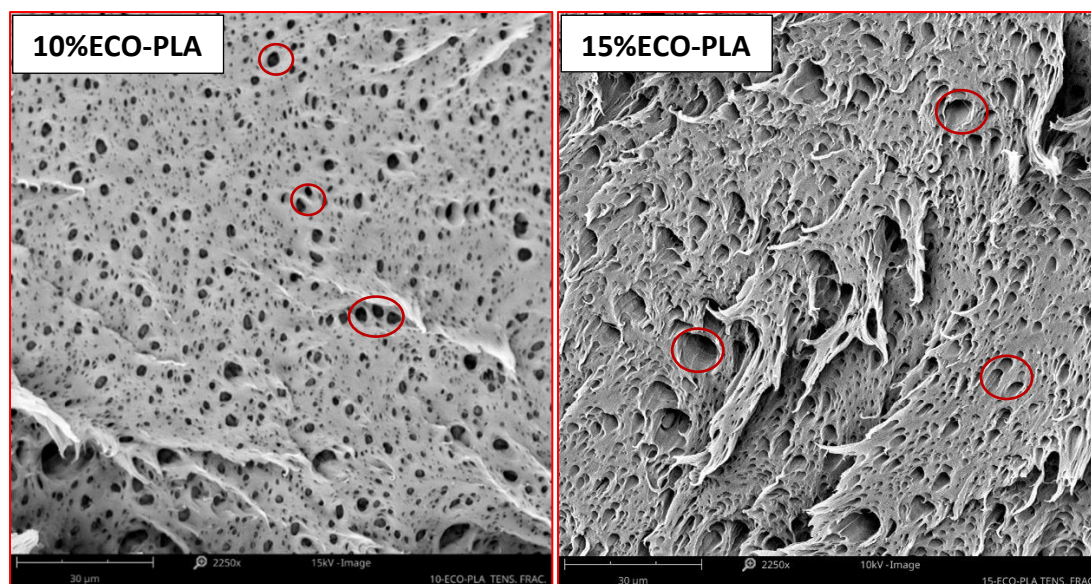


Figure 7: SEM micrographs for tensile fractured surfaces of neat PLA, 5%ECO-PLA, 10%ECO-PLA, and 15%ECO-PLA.

The SEM micrographs of the impact-fractured surfaces, displayed in Figure 8, highlight the gradual influence of ECO on the fracture behavior and mechanisms of PLA. The fracture surface of neat PLA is smooth, with sharp-edged cracks indicative of brittle failure, where rapid crack propagation occurs with minimal energy absorption. This morphology reflects the inherent rigidity and brittleness of PLA, consistent with its low impact strength [65]. With the incorporation of 5% ECO, the fracture surface becomes rougher, with small deformation zones and less pronounced crack propagation, suggesting the onset of ductile behavior. ECO acts as a plasticizer, disrupting the rigid PLA structure and enabling localized chain mobility, resulting in improved energy absorption during impact. At 10% ECO content, the fracture surface exhibits significant roughness, with visible voids, micro-tears, and substantial plastic deformation. These features indicate a clear transition to ductile fracture, where the material effectively dissipates stress and delays crack propagation. The enhanced toughness at this ECO level aligns with the lubricity theory, which posits that ECO reduces friction between polymer chains, and the gel theory, which explains that ECO disrupts strong polymer-polymer interactions, increasing flexibility [53].

At 15% ECO, the fracture surface becomes highly rough and dominated by extensive deformation zones, voids, and fibrillation, indicating maximum energy dissipation and ductile behavior. The increased roughness and deformation zones compared to lower ECO content suggest that the



- 1 material absorbs significant impact energy before failure, although the excessive matrix disruption  
2 at this high ECO content may lead to reduced tensile strength. This behavior is consistent with  
3 findings in the literature, where increasing plasticizer content enhances ductility and toughness but  
4 may compromise the cohesive strength of the polymer matrix [66,67].

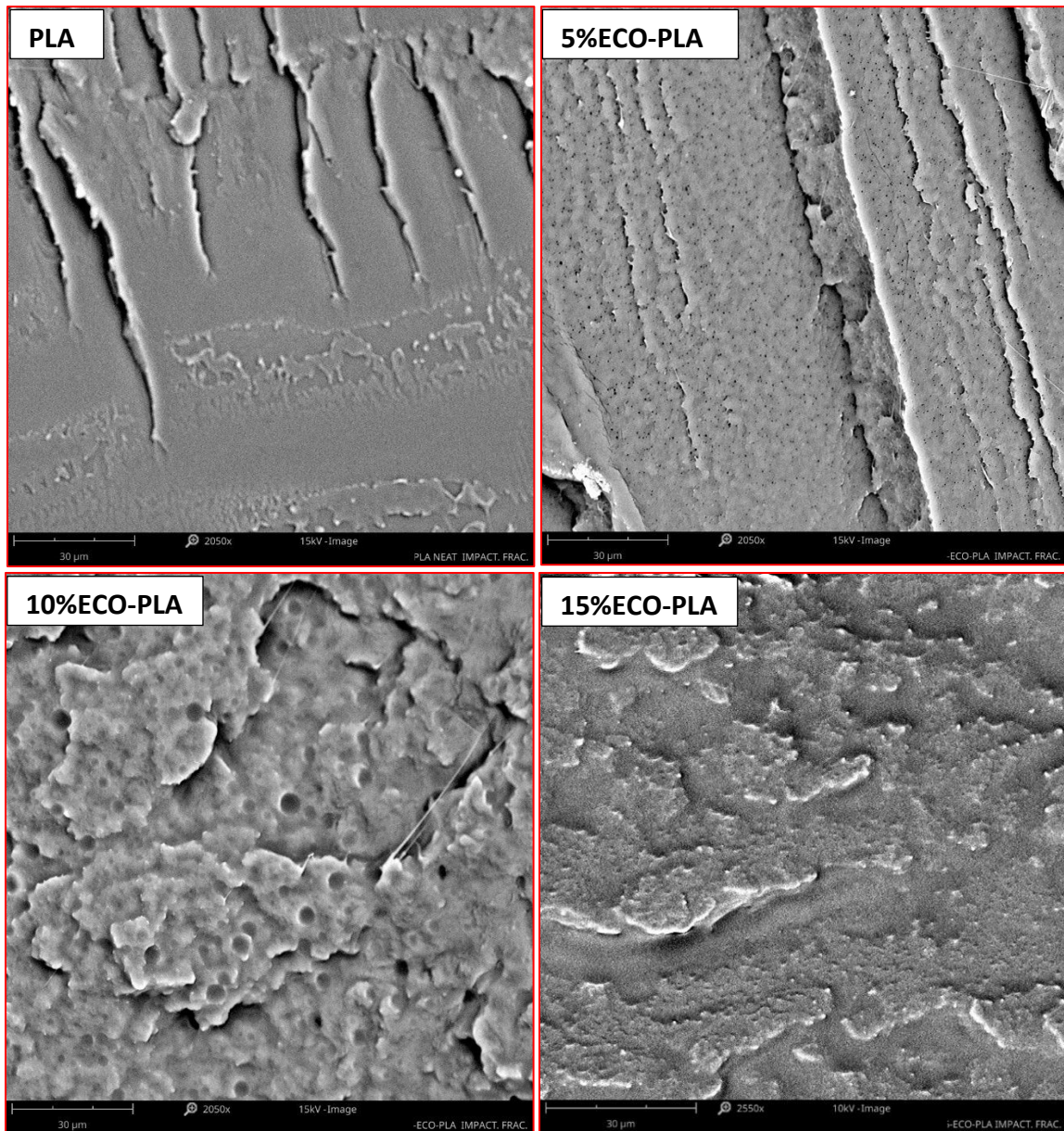


Figure 8: SEM micrographs for impact fractured surfaces of neat PLA, 5% ECO-PLA, 10% ECO-PLA, and 15% ECO-PLA.

## 1 5. Conclusion

2 Camelina oil with high unsaturated contents (90%) was epoxidized by reacting it with hydrogen  
3 peroxide and formic acid, using Amberlite ion exchange resin-H<sup>+</sup> as a catalyst to facilitate the  
4 reaction. NMR spectroscopy validated the epoxidation process by showing the absence of olefinic  
5 proton peaks at 5.3–5.5 ppm and the emergence of oxirane proton peaks in the range of 2.8–3.2  
6 ppm, confirming a high degree of functionalization. FTIR spectroscopy further validated the  
7 chemical modification, with the disappearance of -C=C-H stretching vibrations and the emergence  
8 of characteristic oxirane peaks around 825 cm<sup>-1</sup>. FTIR also revealed shifts in the carbonyl  
9 stretching region of PLA, confirming hydrogen bonding and improved compatibility between ECO  
10 and PLA. The ECO was blended with PLA at various ratios (5%, 10%, and 15%) and evaluated  
11 for its mechanical, thermal, and morphological properties. The inclusion of ECO significantly  
12 enhanced the elongation at break (up to 1680%) and impact strength (up to 25%) of PLA,  
13 transitioning it from brittle to ductile behavior. SEM analysis revealed progressive changes in  
14 fracture morphology, demonstrating enhanced flexibility and toughness. Thermal analysis  
15 indicated a reduction in the T<sub>g</sub>, validating the plasticizing effect of ECO and its role in increasing  
16 polymer chain mobility.

17 The combined insights from NMR and FTIR highlight the successful chemical transformation and  
18 compatibility of ECO with PLA, attributed to the oxirane and hydroxyl groups facilitating strong  
19 intermolecular interactions. These findings underscore the potential of ECO as a renewable and  
20 effective alternative to petroleum-based plasticizers, enhancing the performance of PLA for  
21 applications in packaging, biomedical materials, and other sectors requiring flexibility and  
22 toughness.

### 23 Author Contributions:

24 M.A.: Investigation, Methodology, Data curation, Formal analysis, Visualization, Writing -  
25 Original Draft., Writing—Review and Editing.

26 M. H., Investigation, Methodology, Data curation, Formal analysis, Writing—original Draft  
27 Preparation, Writing—Review and Editing.



1 A. R., Investigation, Methodology, Data curation, Formal analysis, Writing—original Draft  
2 Preparation, Writing—Review and Editing.

3 A. K. M.: Conceptualization, Investigation, Methodology, Validation, Supervision, Resources,  
4 Funding acquisition, Writing - Review & Editing.

5 M. M.: Conceptualization, Investigation, Methodology, Validation, Supervision, Resources,  
6 Funding acquisition, Writing - Review & Editing.

7 All authors contributed to the discussion, reviews and approval of the manuscript for publication.

### 8 **Declaration of competing interest**

9 The authors declare that they have no known competing financial interests or personal  
10 relationships that could have appeared to influence the work reported in this paper.

### 11 **Acknowledgements**

12 This study was financially supported by the Ontario Ministry of Agriculture, Food and Rural  
13 Affairs (OMAFRA) – University of Guelph, the Bioeconomy Industrial Uses Research Program  
14 Theme (Project No. 030706); OMAFRA - Ontario Agri-Food Research Initiative (Project No.  
15 056442); the Natural Sciences and Engineering Research Council of Canada (NSERC), Discovery  
16 Grants Program (Project No. 401716) and the NSERC Canada Research Chair (CRC) Program  
17 Project No. 460788.

18

19

20

21

22

23



## 1 References

- 2 [1] Miyagawa H, Mohanty AK, Misra M, Drzal LT. Thermo-physical and impact properties  
3 of epoxy containing epoxidized linseed oil, 1: Anhydride-cured epoxy. *Macromol Mater*  
4 *Eng* 2004;289:629–35. <https://doi.org/10.1002/MAME.200400004>.
- 5 [2] Miyagawa H, Misra M, Drzal LT, Mohanty AK. Fracture toughness and impact strength  
6 of anhydride-cured biobased epoxy. *Polym Eng Sci* 2005;45:487–95.  
7 <https://doi.org/10.1002/pen.20290>.
- 8 [3] Qin J, Wolcott M, Zhang J. Use of polycarboxylic acid derived from partially  
9 depolymerized lignin as a curing agent for epoxy application. *ACS Sustain Chem Eng*  
10 2014;2:188–93. <https://doi.org/10.1021/sc400227v>.
- 11 [4] ASTM. ASTM D6400-21, Standard Specification for Labeling of Plastics Designed to be  
12 Aerobically Composted in Municipal or Industrial Facilities 2022:3.  
13 <https://doi.org/10.1520/D6400-23>.
- 14 [5] Bhardwaj R, Mohanty AK. Advances in the Properties of Polylactides Based Materials: A  
15 Review. *J Biobased Mater Bioenergy* 2008;1:191–209.  
16 <https://doi.org/10.1166/jbmb.2007.023>.
- 17 [6] Wu N, Zhang H, Fu G. Super-tough Poly(lactide) Thermoplastic Vulcanizates Based on  
18 Modified Natural Rubber 2016. <https://doi.org/10.1021/acssuschemeng.6b02197>.
- 19 [7] Garlotta D. A Literature Review of Poly(Lactic Acid). vol. 9. 2001.
- 20 [8] Ren W, Pan X, Wang G, Cheng W, Liu Y. Dodecylated lignin-: G -PLA for effective  
21 toughening of PLA. *Green Chem* 2016;18:5008–14. <https://doi.org/10.1039/c6gc01341d>.



- 1 [9] Mauck SC, Wang S, Ding W, Rohde BJ, Fortune CK, Yang G, et al. Biorenewable Tough  
2 Blends of Polylactide and Acrylated Epoxidized Soybean Oil Compatibilized by a  
3 Polylactide Star Polymer. *Macromolecules* 2016;49:1605–15.  
4 <https://doi.org/10.1021/acs.macromol.5b02613>.
- 5 [10] Zhao X, Hu H, Wang X, Yu X, Zhou W, Peng S. Super tough poly(lactic acid) blends: A  
6 comprehensive review. *RSC Adv* 2020;10:13316–68. <https://doi.org/10.1039/d0ra01801e>.
- 7 [11] Liu H, Zhang J. Research progress in toughening modification of poly(lactic acid). *J*  
8 *Polym Sci Part B Polym Phys* 2011;49:1051–83. <https://doi.org/10.1002/polb.22283>.
- 9 [12] Murariu M, Paint Y, Murariu O, Laoutid F, Dubois P. Tailoring and Long-Term  
10 Preservation of the Properties of PLA Composites with “Green” Plasticizers. *Polymers*  
11 *(Basel)* 2022;14. <https://doi.org/10.3390/polym14224836>.
- 12 [13] Tábi T, Ageyeva T, Kovács JG. Improving the ductility and heat deflection temperature of  
13 injection molded Poly(lactic acid) products: A comprehensive review. *Polym Test*  
14 2021;101. <https://doi.org/10.1016/j.polymertesting.2021.107282>.
- 15 [14] Sun S, Weng Y, Zhang C. Recent advancements in bio-based plasticizers for polylactic  
16 acid ( PLA ): A review. *Polym Test* 2024;140:108603.  
17 <https://doi.org/10.1016/j.polymertesting.2024.108603>.
- 18 [15] Kfoury G, Raquez JM, Hassouna F, Odent J, Toniazzo V, Ruch D, et al. Recent advances  
19 in high performance poly(lactide): From “green” plasticization to super-tough materials  
20 via (reactive) compounding. *Front Chem* 2013;1:1–46.  
21 <https://doi.org/10.3389/fchem.2013.00032>.



- 1 [16] Sun S, Weng Y, Han Y, Zhang C. Plasticization mechanism of biobased plasticizers  
2 comprising polyethylene glycol diglycidyl ether-butyl citrate with both long and short  
3 chains on poly(lactic acid). *Int J Biol Macromol* 2024;276:133948.  
4 <https://doi.org/10.1016/j.ijbiomac.2024.133948>.
- 5 [17] Valerio O, Pin JM, Misra M, Mohanty AK. Synthesis of glycerol-based biopolyesters as  
6 toughness enhancers for polylactic acid bioplastic through reactive extrusion. *ACS Omega*  
7 2016;1:1284–95. <https://doi.org/10.1021/acsomega.6b00325>.
- 8 [18] Xia Y, Larock RC. Vegetable oil-based polymeric materials: Synthesis, properties, and  
9 applications. *Green Chem* 2010;12:1893–909. <https://doi.org/10.1039/c0gc00264j>.
- 10 [19] Mehta G, Mohanty AK, Misra M, Drzal LT. Biobased resin as a toughening agent for  
11 biocomposites. *Green Chem* 2004;6:254–8. <https://doi.org/10.1039/b316658a>.
- 12 [20] Al-Mulla EAJ, Yunus WMZW, Ibrahim NAB, Rahman MZA. Properties of epoxidized  
13 palm oil plasticized poly(lactic acid). *J Mater Sci* 2010;45:1942–6.  
14 <https://doi.org/10.1007/s10853-009-4185-1>.
- 15 [21] Quiles-Carrillo L, Duart S, Montanes N, Torres-Giner S, Balart R. Enhancement of the  
16 mechanical and thermal properties of injection-molded polylactide parts by the addition of  
17 acrylated epoxidized soybean oil. *Mater Des* 2018;140:54–63.  
18 <https://doi.org/10.1016/j.matdes.2017.11.031>.
- 19 [22] Valerio O, Misra M, Mohanty AK. Poly(glycerol- co-diacids) Polyesters: From Glycerol  
20 Biorefinery to Sustainable Engineering Applications, A Review. *ACS Sustain Chem Eng*  
21 2018;6:5681–93. <https://doi.org/10.1021/acssuschemeng.7b04837>.



- 1 [23] Mashouf Roudsari G, Mohanty AK, Misra M. Study of the curing kinetics of epoxy resins  
2 with biobased hardener and epoxidized soybean oil. *ACS Sustain Chem Eng*  
3 2014;2:2111–6. <https://doi.org/10.1021/sc500176z>.
- 4 [24] Carbonell-Verdu A, Garcia-Garcia D, Dominici F, Torre L, Sanchez-Nacher L, Balart R.  
5 PLA films with improved flexibility properties by using maleinized cottonseed oil. *Eur*  
6 *Polym J* 2017;91:248–59. <https://doi.org/10.1016/j.eurpolymj.2017.04.013>.
- 7 [25] Quiles-Carrillo L, Blanes-Martínez MM, Montanes N, Fenollar O, Torres-Giner S, Balart  
8 R. Reactive toughening of injection-molded polylactide pieces using maleinized hemp  
9 seed oil. *Eur Polym J* 2018;98:402–10. <https://doi.org/10.1016/j.eurpolymj.2017.11.039>.
- 10 [26] Ferri JM, Garcia-Garcia D, Sánchez-Nacher L, Fenollar O, Balart R. The effect of  
11 maleinized linseed oil (MLO) on mechanical performance of poly(lactic acid)-  
12 thermoplastic starch (PLA-TPS) blends. *Carbohydr Polym* 2016;147:60–8.  
13 <https://doi.org/10.1016/j.carbpol.2016.03.082>.
- 14 [27] Liu W, Qiu J, Fei ME, Qiu R, Sakai E. Manufacturing of Thermally Remoldable Blends  
15 from Epoxidized Soybean Oil and Poly(lactic acid) via Dynamic Cross-Linking in a Twin-  
16 Screw Extruder. *Ind Eng Chem Res* 2018;57:7516–24.  
17 <https://doi.org/10.1021/acs.iecr.8b01189>.
- 18 [28] Miyagawa H, Misra M, Drzal LT, Mohanty AK. Novel biobased nanocomposites from  
19 functionalized vegetable oil and organically-modified layered silicate clay. *Polymer*  
20 (Guildf) 2005;46:445–53. <https://doi.org/10.1016/j.polymer.2004.11.031>.
- 21 [29] Zanetti F, Alberghini B, Marjanovi A, Grahovac N, Rajkovi D, Kiproviski B, et al.  
22 Camelina , an ancient oilseed crop actively contributing to the rural renaissance in Europe



- 1 . A review 2021.
- 2 [30] Slavova-Kazakova, A., Marcheva, M., Taneva, S. and Momchilova S. Oxidative Stability  
3 of the Oil from Camelina (*Camelina sativa* L.) Seeds: Effects of Ascorbyl Palmitate  
4 Concentrations. *Seeds* 2025;4:38.
- 5 [31] Arshad M, Mohanty AK, Van Acker R, Riddle R, Todd J, Khalil H, et al. Valorization of  
6 camelina oil to biobased materials and biofuels for new industrial uses: a review. *RSC*  
7 *Adv* 2022;12:27230–45. <https://doi.org/10.1039/d2ra03253h>.
- 8 [32] Arshad M, Shankar S, Mohanty AK, Todd J, Riddle R, Van Acker R, et al. Improving the  
9 Barrier and Mechanical Properties of Paper Used for Packing Applications with  
10 Renewable Hydrophobic Coatings Derived from Camelina Oil. *ACS Omega*  
11 2024;9:19786–95. <https://doi.org/10.1021/acsomega.3c07213>.
- 12 [33] Safder M, Arshad M, Temelli F, Ullah A. Bio-composites from spent hen derived lipids  
13 grafted on CNC and reinforced with nanoclay. *Carbohydr Polym* 2022;281:119082.  
14 <https://doi.org/10.1016/j.carbpol.2021.119082>.
- 15 [34] ASTM INTERNATIONAL. Standard Test Method for Tensile Properties of Plastics  
16 (ASTM D638). vol. 08. 2014.
- 17 [35] ASTM INTERNATIONAL. Standard Test Methods for Flexural Properties of  
18 Unreinforced and Reinforced Plastics and Electrical Insulating Materials. D790. *Annu B*  
19 *ASTM Stand* 2002:1–12. <https://doi.org/10.1520/D0790-17.2>.
- 20 [36] ASTM Standard D256. Standard Test Methods for Determining the Izod Pendulum  
21 Impact Resistance of Plastics. *ASTM Int* 2010. <https://doi.org/10.1520/D0256-24.2>.



- 1 [37] Bach QV, Vu CM, Vu HT, Hoang T, Dieu TV, Nguyen DD. Epoxidized soybean oil  
2 grafted with CTBN as a novel toughener for improving the fracture toughness and  
3 mechanical properties of epoxy resin. *Polym J* 2020;52:345–57.  
4 <https://doi.org/10.1038/s41428-019-0275-3>.
- 5 [38] Mahadi MB, Azmi IS, Ahmad MA, Rahim NH, Jalil MJ. Catalytic epoxidation of  
6 sunflower oil derived by linoleic acid via in situ peracid mechanism. *Biomass Convers*  
7 *Biorefinery* 2024. <https://doi.org/10.1007/s13399-024-05658-3>.
- 8 [39] Balanuca B, Stan R, Lungu A, Vasile E, Iovu H. Hybrid networks based on epoxidized  
9 camelina oil. *Des Monomers Polym* 2017;20:10–7.  
10 <https://doi.org/10.1080/15685551.2016.1231031>.
- 11 [40] Giita Silverajah VS, Ibrahim NA, Zainuddin N, Wan Yunus WMZ, Hassan HA.  
12 Mechanical, thermal and morphological properties of poly(lactic acid)/epoxidized palm  
13 olein blend. *Molecules* 2012;17:11729–47. <https://doi.org/10.3390/molecules171011729>.
- 14 [41] Chieng BW, Ibrahim NA, Then YY, Loo YY. Epoxidized vegetable oils plasticized  
15 poly(lactic acid) biocomposites: Mechanical, thermal and morphology properties.  
16 *Molecules* 2014;19:16024–38. <https://doi.org/10.3390/molecules191016024>.
- 17 [42] Bouti M, Irinislimane R, Belhaneche-Bensemra N. Properties Investigation of Epoxidized  
18 Sunflower Oil as Bioplasticizer for Poly (Lactic Acid). *J Polym Environ* 2022;30:232–45.  
19 <https://doi.org/10.1007/s10924-021-02194-3>.
- 20 [43] Films B. Epoxidized Soybean Oil Toughened Poly(lactic acid)/Lignin-g-Poly(lauryl  
21 methacrylate) Bio-Composite Films with Potential Food Packaging Application. *Polymers*  
22 (Basel) 2024;16.



- 1 [44] Siudem P, Zielińska A, Paradowska K. Application of <sup>1</sup>H NMR in the study of fatty acids  
2 composition of vegetable oils. *J Pharm Biomed Anal* 2022;212:1–8.  
3 <https://doi.org/10.1016/j.jpba.2022.114658>.
- 4 [45] Alexandri E, Ahmed R, Siddiqui H, Choudhary MI, Tsiafoulis CG, Gerothanassis IP.  
5 High resolution NMR spectroscopy as a structural and analytical tool for unsaturated  
6 lipids in solution. *Molecules* 2017;22. <https://doi.org/10.3390/molecules22101663>.
- 7 [46] Çaylı G, Cekli S, Uzunoğlu CP. Synthesis, photopolymerization and evaluation of  
8 electrical properties of epoxidized castor oil-based acrylates. *Polym Bull* 2024;81:13289–  
9 304. <https://doi.org/10.1007/s00289-024-05349-z>.
- 10 [47] Akintayo Emmanuel T, Akintayo Cecilia O, Oluwaleye IO, Ajaja O, Beuermann S.  
11 Synthesis and characterization of azidated *Adenopus breviflorus* benth seed oil. *Green*  
12 *Chem Lett Rev* 2020;13:115–26. <https://doi.org/10.1080/17518253.2020.1737251>.
- 13 [48] Thuy NT, Lan PN. Investigation of the impact of two types of epoxidized vietnam rubber  
14 seed oils on the properties of polylactic acid. *Adv Polym Technol* 2021;2021.  
15 <https://doi.org/10.1155/2021/6698918>.
- 16 [49] Maiza M, Benaniba MT, Quintard G, Massardier-Nageotte V. Biobased additive  
17 plasticizing Polylactic acid (PLA). *Polimeros* 2015;25:581–90.  
18 <https://doi.org/10.1590/0104-1428.1986>.
- 19 [50] Farrag Y, Barral L, Gualillo O, Moncada D, Rico M, Bouza R. Effect of Different  
20 Plasticizers on Thermal, Crystalline, and Permeability Properties. *Polymers (Basel)*  
21 2022;14.



- 1 [51] Li D, Jiang Y, Lv S, Liu X, Gu J, Chen Q, et al. Preparation of plasticized poly (lactic  
2 acid) and its influence on the properties of composite materials. PLoS One 2018;13:1–15.  
3 <https://doi.org/10.1371/journal.pone.0193520>.
- 4 [52] Bocqué M, Voirin C, Lapinte V, Caillol S, Robin JJ. Petro-based and bio-based  
5 plasticizers: Chemical structures to plasticizing properties. J Polym Sci Part A Polym  
6 Chem 2016;54:11–33. <https://doi.org/10.1002/pola.27917>.
- 7 [53] Eslami Z, Elkoun S, Robert M, Adjallé K. A Review of the Effect of Plasticizers on the  
8 Physical and Mechanical Properties of Alginate-Based Films. Molecules 2023;28.  
9 <https://doi.org/10.3390/molecules28186637>.
- 10 [54] Guo J, Wang J, He Y, Sun H, Chen X, Zheng Q, et al. Triply biobased thermoplastic  
11 composites of polylactide/succinylated lignin/epoxidized soybean oil. Polymers (Basel)  
12 2020;12. <https://doi.org/10.3390/polym12030632>.
- 13 [55] Wasti S, Triggs E, Farag R, Auad M, Adhikari S, Bajwa D, et al. Influence of plasticizers  
14 on thermal and mechanical properties of biocomposite filaments made from lignin and  
15 polylactic acid for 3D printing. Compos Part B Eng 2021;205.  
16 <https://doi.org/10.1016/j.compositesb.2020.108483>.
- 17 [56] Daniels PH. A brief overview of theories of PVC plasticization and methods used to  
18 evaluate PVC-plasticizer interaction. J Vinyl Addit Technol 2009;15:219–23.  
19 <https://doi.org/10.1002/vnl.20211>.
- 20 [57] Xie J, Gu K, Zhao Y, Yao J, Chen X, Shao Z. Enhancement of the Mechanical Properties  
21 of Poly(lactic acid)/Epoxidized Soybean Oil Blends by the Addition of 3-  
22 Aminophenylboronic Acid. ACS Omega 2022;7:17841–8.



- 1 <https://doi.org/10.1021/acsomega.2c01102>.
- 2 [58] Zhao TH, Yuan WQ, Li YD, Weng YX, Zeng JB. Relating Chemical Structure to  
3 Toughness via Morphology Control in Fully Sustainable Sebacic Acid Cured Epoxidized  
4 Soybean Oil Toughened Polylactide Blends. *Macromolecules* 2018;51:2027–37.  
5 <https://doi.org/10.1021/acs.macromol.8b00103>.
- 6 [59] Orue A, Eceiza A, Arbelaiz A. Preparation and characterization of poly(lactic acid)  
7 plasticized with vegetable oils and reinforced with sisal fibers. *Ind Crops Prod*  
8 2018;112:170–80. <https://doi.org/10.1016/j.indcrop.2017.11.011>.
- 9 [60] Tee YB, Talib RA, Abdan K, Chin NL, Basha RK, Yunus KFM. Toughening Poly(Lactic  
10 Acid) and Aiding the Melt-compounding with Bio-sourced Plasticizers. *Agric Agric Sci*  
11 *Procedia* 2014;2:289–95. <https://doi.org/10.1016/j.aaspro.2014.11.041>.
- 12 [61] Lazaro-Hdez, C., Valerga, A.P., Gomez-Carturla, J., Sanchez-Nacher, L., Boronat, T. and  
13 Ivorra-Martinez J. Optimization of the ductile properties of poly(lactic acid) (PLA) using  
14 green citrate-based plasticizers and itaconic anhydride grafted PLA (PLA-g-IA). *Int J Biol*  
15 *Macromol* 2025;307:142034. <https://doi.org/10.1016/j.ijbiomac.2025.142034>.
- 16 [62] Chieng, B.W., Ibrahim, N.A., Then, Y.Y. and Loo YY. Mechanical, thermal, and  
17 morphology properties of poly (lactic acid) plasticized with poly (ethylene glycol) and  
18 epoxidized palm oil hybrid plasticizer. *Polym Eng Sci* 2016;56:1169–74.  
19 <https://doi.org/10.1002/pen>.
- 20 [63] Balart LNPCNAOJGOFr. Plasticization of Polylactide Using Biobased Epoxidized  
21 Isobutyl Esters Derived from Waste Soybean Oil Deodorizer Distillate. *J Polym Environ*  
22 2025;33:125–44.



- 1 [64] Tejada-Oliveros R, Balart R, Ivorra-Martinez J, Gomez-Caturla J, Montanes N, Quiles-  
2 Carrillo L. Improvement of Impact Strength of Polylactide Blends with a Thermoplastic  
3 Elastomer Compatibilized with Biobased Maleinized Linseed Oil for Applications in  
4 Rigid Packaging. *Molecules* 2021;26. <https://doi.org/10.3390/MOLECULES26010240>.
- 5 [65] Gao H, Qiang T. Fracture surface morphology and impact strength of cellulose/PLA  
6 composites. *Materials (Basel)* 2017;10:1–11. <https://doi.org/10.3390/ma10060624>.
- 7 [66] Pradhan DK, Samantaray BK, Choudhary RNP, Thakur AK. Effect of plasticizer on  
8 structure - Property relationship in composite polymer electrolytes. *J Power Sources*  
9 2005;139:384–93. <https://doi.org/10.1016/j.jpowsour.2004.05.050>.
- 10 [67] Minale YF, Gajdoš I, Štef P, Szabó T, Kovács AP, Major AÁ, et al. Mechanical  
11 Properties of PVC / TPU Blends Enhanced with a Sustainable Bio-Plasticizer 2025.  
12  
13

